A Power Electronic Transformer for PWM AC Drive with Lossless Commutation and Common-mode Voltage Suppression

Kaushik Basu, Member, *IEEE* and Ned Mohan Fellow, *IEEE*
Department of Electrical and Computer Engineering
University of Minnesota
Minneapolis, Minnesota 55455
Email: basux017@umn.edu

***Abstract*—This paper presents a novel dc/ac converter topology with a high frequency transformer-link for three-phase adjustable magnitude and frequency PWM ac drives. Such drives find wide range of applications including UPS systems and drives involving renewable energy sources like solar and fuel cells. One recent potential area of application is renewable energy sources like wind or wave connected with HVDC grid. Here power conversion is single stage and bidirectional. Use of high frequency transformer results in high power density. The proposed topology minimizes the number of switching transitions between the transformer winding and the load and hence reduces common-mode voltage switching and improves the quality of the output voltage waveform. A novel modulation technique presented in this paper results in minimum common-mode voltage switching. A lossless source based commutation method has been developed to commute the energy stored in the leakage inductances of the high frequency transformer. This method also results in soft switching (ZCS) of all four-quadrant switches in the load side converter. The proposed converter has been analyzed and simulated. The presented simulation results verify the operation of the proposed topology.**

I. Introduction

An inverter with high frequency transformer-link finds applications in standby power supplies like UPS systems along with renewable energy sources like photovoltaic and fuel cells [1] [2]. One recent interesting area of application is wind power systems connected to high voltage dc grid (HVDC). A transformer provides necessary galvanic isolation and required voltage transfer ratio. Use of high frequency transformer results in high power density by reducing the size and weight of the magnetics.

A conventional system has multiple-stages of power conversion (dc-high frequency ac-dc-adjustable ac) and requires electrolytic dc capacitors that reduces the reliability of the system. Systems, capable of more direct power conversion, can generally be classified as either resonant or non-resonant/PWM converters. Resonant converters contain reactive elements and their output voltage depends on loading [3] [4]. Non-resonant converters use the conventional PWM control of ac drives. These PWM type of converters practically do not need any storage elements.

This work is supported by office of Naval Research, Grant N 00014-07-1-0968. The financial support is gratefully acknowledged.

Single-phase dc/ac inverter with high frequency ac-link are analyzed in [5] [6]. When the output current and voltage are in the same quadrant, this converter can be operated like a phase-modulated full-bridge converter in order to get soft switching in most of the switches [7].

A three-phase dc/ac inverter with high frequency ac-link was first proposed in [6]. The H-bridge in the primary or dc voltage side of the system converts the input dc voltage to a high frequency 50 % duty cycle square wave ac voltage. The output cycloconverter converts the high frequency ac voltage to a variable magnitude and frequency PWM output voltage. In [8], it has been identified that since the three-phase load is generally inductive, every time the output cycloconverter switches, the energy stored in the leakage inductances of the transformer needs to be commutated. A source-based commutation of the leakage energy is presented in [8]. In [3], an auxiliary circuit and control method has been developed in order to get soft switching. In [2], a carrier based PWM technique has been presented for the secondary side converter.

Any switching of the secondary side cycloconverter requires commutation of leakage energy and results in the loss of output voltage [3], distortion in the load current and common-mode voltage switching. Also the source based commutation process in [8] requires a sequence of complicated switching at variable instants of time. If conventional space vector PWM (CSVPWM) is employed to modulate the output cycloconverter then it changes its switching state six times in a subcycle over which the average output voltage vector is synthesized.

In [9] an alternative topology has been proposed where the PWM voltage is synthesized in the input two level converter and output consists of three square wave modulated cycloconverters. This topology minimizes the switching transitions between the transformer leakage inductance and the output inductive load. Leakage energy needs to be commutated only once in a subcycle. One of the important feature of a modern PWM ac drive is common-mode voltage elimination, [10]. In this topology common-mode voltage elimination is possible at the cost the quality of the output voltage waveform.

This paper presents a topology (Fig. 1) where six voltage vectors that result in zero common-mode voltage are available

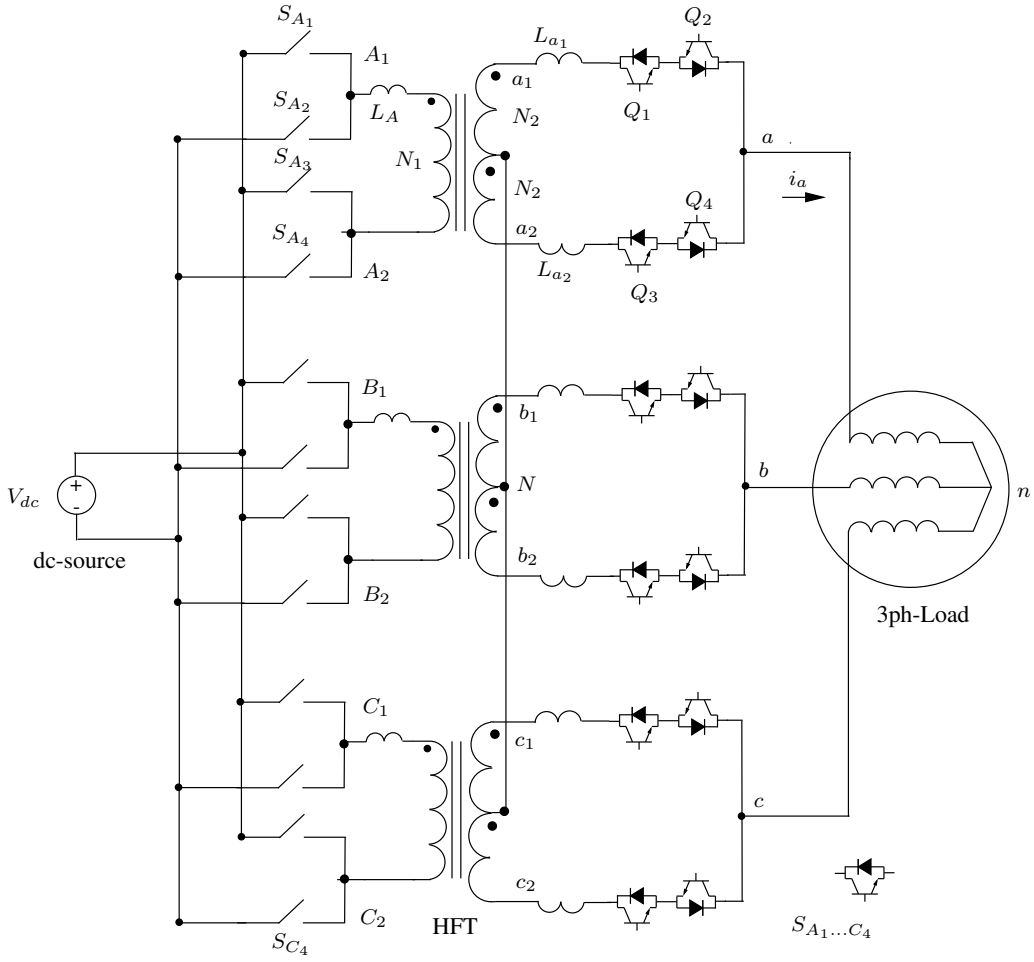

Fig. 1. Circuit diagram of the proposed topology

for modulation (similar to a two level inverter). So modulation with these vectors results in high quality output voltage waveform. Also the lossless source based commutation process is simpler compared to [9]. In this topology, availability of more voltage (in comparison with [9]) for leakage energy commutation results in lower commutation time, higher frequency of operation and high power density. In this converter commutation is done when modulation of the output voltage vector requires an application of zero vector. This results in less amount of output voltage loss during commutation. The advantages of the proposed converter are:

1) Step change in voltage level, isolation and high power density
2) Common-mode voltage suppression
3) A simple lossless commutation of leakage energy
4) Minimization of output voltage loss
5) High quality output voltage waveform
6) Single-stage power conversion (no storage element) with bidirectional power flow capability
7) Soft-switching

II. Analysis

The control of this converter is divided into two parts: modulation or the power transfer and commutation. The various control signals are given in Fig. 2. Modulation of this topology has two stages and controlled by the signal S. In the first half of modulation when the signal S goes high the power is transferred through the upper half of the secondary windings of the three high frequency transformers. During the next half when signal S goes low, power is transferred through the lower half of the secondary windings. Commutation happens when power flow changes from one stage to the consecutive one. During commutation signals C_1 or C_2 goes high.

A. Modulation

During each stages of modulation the required (adjustable frequency and magnitude) three phase output voltages are synthesized on an average at the load terminals. (1) gives the expressions of these three phase balanced voltages. V_o is the magnitude and ω_o is the frequency of the average output voltage. The definition of the output voltage space vector $\mathbf{V_o}$ is given by (2). In (3) $\mathbf{V_{ref}}$ is the reference or the average output voltage space vector. Using (1) $\mathbf{V_{ref}}$ turns out to be a constant magnitude ($\frac{3}{2}V_o$) synchronously rotating

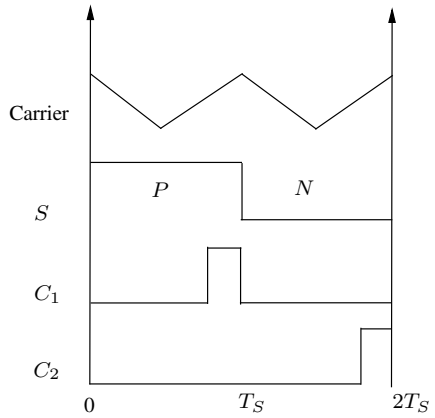

Fig. 2. Control Signals

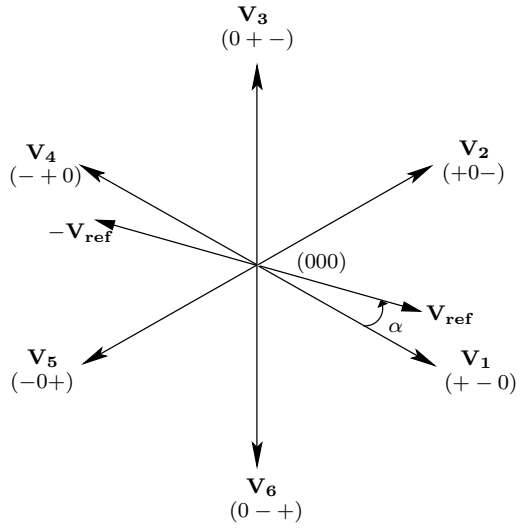

Fig. 3. available voltage space vectors with zero common mode voltage

space vector rotating at the speed ω_o. (4) defines the voltage space vector for the voltages induced in the upper half of the secondary windings. These voltages are measured with respect to the star point N formed by the mid points of the secondary windings. Similarly (5) provides the definition of the voltage space vectors formed by the voltages induced in the lower half of the secondary winding. In (6) $\mathbf{V_p}$ refers to the voltage space vector formed by the primary side voltages of the three high frequency transformers. N_1 is the number of turns of the primary winding of each of the transformers. N_2 is the number of turns of each half of the secondary windings. During modulation or power transfer stage we can neglect the voltage drop in the leakage impedances of the transformer. This implies (7) holds. Using (4), (5), (6) and (7) it is possible to obtain (8).

$$\begin{aligned} \overline{v_{an}} &= V_o \cos(\omega_o t) \\ \overline{v_{bn}} &= V_o \cos\left(\omega_o t - \frac{2\pi}{3}\right) \\ \overline{v_{cn}} &= V_o \cos\left(\omega_o t + \frac{2\pi}{3}\right) \end{aligned} \tag{1}$$

$$\mathbf{V_o} = v_{an} + v_{bn} e^{j\frac{2\pi}{3}} + v_{cn} e^{-j\frac{2\pi}{3}} \tag{2}$$

$$\begin{aligned} \mathbf{V_{ref}} &= \overline{v_{an}} + \overline{v_{bn}} e^{j\frac{2\pi}{3}} + \overline{v_{cn}} e^{-j\frac{2\pi}{3}} \\ &= \frac{3}{2} V_o e^{j\omega_o t} \end{aligned} \tag{3}$$

$$\mathbf{V_{s_1}} = v_{a_1N} + v_{b_1N} e^{j\frac{2\pi}{3}} + v_{c_1N} e^{-j\frac{2\pi}{3}} \tag{4}$$

$$\mathbf{V_{s_2}} = v_{a_2N} + v_{b_2N} e^{j\frac{2\pi}{3}} + v_{c_2N} e^{-j\frac{2\pi}{3}} \tag{5}$$

$$\mathbf{V_p} = v_{A_1A_2} + v_{B_1B_2} e^{j\frac{2\pi}{3}} + v_{C_1C_2} e^{-j\frac{2\pi}{3}} \tag{6}$$

$$\begin{aligned} v_{a_1N} &= -v_{a_2N} = \left(\frac{N_2}{N_1}\right) v_{A_1A_2} \\ v_{b_1N} &= -v_{b_2N} = \left(\frac{N_2}{N_1}\right) v_{B_1B_2} \\ v_{c_1N} &= -v_{c_2N} = \left(\frac{N_2}{N_1}\right) v_{C_1C_2} \end{aligned} \tag{7}$$

$$\mathbf{V_{s_1}} = -\mathbf{V_{s_2}} = \left(\frac{N_2}{N_1}\right) \mathbf{V_p} \tag{8}$$

In the first half of the modulation only the upper half of the secondary windings conduct. For example during this stage in Fig. 1 in phase a the switches Q_1 and Q_2 are ON and Q_3 and Q_4 are OFF. So when S goes high as the load is considered to be balanced and neutral point n is floating, $\mathbf{V_o}$ is equal to $\left(\frac{N_2}{N_1}\right)\mathbf{V_p}$. Note that in each phase the primary winding of the transformer is connected to the dc-bus with a H-bridge. For example in phase a this bridge consists of four two quadrant switches S_{A_1} to S_{A_4}. In each leg the switches are controlled in a complementary fashion in order to avoid short circuit of the input voltage source and interruption of the output inductive load current. For example at any instant of time either of the switches S_{A_1} or S_{A_2} is ON but they are never turned on simultaneously. Considering this switching strategy each H bridge has four switching states. Two of them are active. During these states the possible applied primary voltages (v_p)

TABLE I
SWITCHING STATES

State	0	+	−	0
S_1	ON	ON	OFF	OFF
S_3	ON	OFF	ON	OFF
v_p	0	V_{dc}	$-V_{dc}$	0

are $+V_{dc}$ or $-V_{dc}$. Rest of the two are zero states i.e. the primary winding is short circuited. These states are given in Table I. In this analysis the positive active state of a bridge is denoted by +, negative state is by - and zero state is by 0. As each bridge has three different states all the three bridges can apply 27 possible voltage combinations to the three phase load. Out of these possibilities here only six active states are considered that leads to zero common mode voltage at the load terminals. For example when a phase bridge applies a positive voltage, b phase bridge applies a negative voltage and c phase bridge applies zero voltage the sum of the three voltages is zero. In this discussion this particular switching state is referred as $(+-0)$. This six active states produces six active voltage vectors at the primary terminals. This vectors, scaled with $\left(\frac{N_2}{N_1}\right)$, is given in Fig. 3. The state $(+-0)$ generates voltage vector $\mathbf{V_1}$. As in this state $V_{A_1A_2} = V_{dc}$, $V_{B_1B_2} = -V_{dc}$ and $V_{C_1C_2} = 0$, by (6) $\mathbf{V_p} = V_{dc}\sqrt{3}e^{-j\frac{\pi}{6}}$ and $\mathbf{V_1} = \mathbf{V_p}\left(\frac{N_2}{N_1}\right)$. Similarly it is possible to obtain other five active voltage vectors as shown in Fig. (3).

In the first half of the power transfer the output reference voltage vector, $\mathbf{V_{ref}}$, is synthesized by using these six active voltage vectors and the zero vectors. This situation is similar to a two level voltage source inverter. The 6 active space vectors divide the complex plane into six symmetrical sectors. The output voltage vector is generated by using the two active vectors that form the sector in which the output reference voltage is located at that particular instant of time. For example in Fig. 3, the reference voltage vector is synthesized on an average using vectors $\mathbf{V_1}$ and $\mathbf{V_2}$, (9). The duty ratios (d_1 and d_2) or the fraction of time for which these active vectors need to be applied are given in (10). Here m is the modulation index and is equal to $\dfrac{V_{ref}}{V_{dc}\left(\frac{N_2}{N_1}\right)}$.

During the second half of the modulation power is transferred through the lower half of the secondary windings. During this state $\mathbf{V_o}$ is equal to the negative of $\left(\dfrac{N_2}{N_1}\right)\mathbf{V_p}$. So in this stage the negative of the output reference voltage vector is generated using six available active voltage space vectors, Fig. (3). As the three high frequency transformers are identical the magnetizing inductances forms a balanced three phase load at the primary side. Over one full cycle of modulation the net average voltage vector applied to the magnetizing inductances is zero. This results in flux balance in the cores of the three high frequency transformers.

$$\mathbf{V_{ref}} = d_1\mathbf{V_1} + d_2\mathbf{V_2} \tag{9}$$

$$\begin{aligned} d_1 &= m\sin\left(\frac{\pi}{3} - \alpha\right) \\ d_2 &= m\sin\alpha \end{aligned} \tag{10}$$

B. Commutation

Commutation happens at each transition of the signal S-low to high or high to low. Commutation refers to the following processes 1) change in the direction of the current in the primary leakage inductance (L_A) 2) exchange of the output current between the leakage inductances (L_{a_1} and L_{a_2}) of the two halves of the secondary winding. Commutation is done on a per phase basis by applying a voltage in the proper direction ($+V_{dc}$ or $-V_{dc}$) across the primary winding and controlling the individual igbts ($Q_{1,2,3,4}$) in the secondary side converter. Depending on the sign of the output current and two possible transitions of S, four cases are possible. The switching scheme for $Q_{1,2,3,4}$ and the required primary voltage is given in Table II and III for all of these four cases. Here, the case when output current is positive and S is making a transition from high to low is described in detail. This implies initially power was flowing through the upper half of the primary winding. Fig. 4(a), depicts the circuit just before C_1 goes high. The commutation stage is given in Fig. 4(b). From Table II a negative voltage ($-V_{dc}$) is required to be applied at the transformer primary. Application of this voltage and turning ON of Q_3 (at zero current) forward biases diode D_4. In this analysis magnetizing currents are neglected. According to transformer relationships (11) and (12) are true. I_a is the value of i_a at this instant of time. Here it is assumed that i_a appears to be a current source in this analysis. This is because commutation happens in a period of time that is much smaller than time period of the output current. By KCL at point a we get (13). Application of KVL on primary and secondary windings leads to (14) and (15). Solving of these equations we get (16). The commutation time is maximum when the output current is at its peak (I_o). The time period for which C_1 and C_2 is high is chosen to be equal to t_{com}, (17). When i_{a_2} reaches I_a, i_{a_1} and i_A becomes $-I_a$ and zero respectively and the commutation process comes to a natural end. When C_1 goes low Q_1 is switched OFF and Q_4 is turned ON at zero current (ZCS). Fig. 4(c) depicts the circuit configuration after the commutation process is completed.

TABLE II
$i_o > 0$

	Q_1	Q_2	Q_3	Q_4	D_1	D_2	D_3	D_4	V_p
P	1	X	0	0	0	1	0	0	X
C_1	1	0	1	0	0	1	0	1	$-V_{dc}$
N	0	0	1	X	0	0	0	1	X
C_2	1	0	1	0	0	1	0	1	V_{dc}

TABLE III
$i_o < 0$

	Q_1	Q_2	Q_3	Q_4	D_1	D_2	D_3	D_4	V_p
P	X	1	0	0	1	0	0	0	X
C_1	0	1	0	1	1	0	1	0	V_{dc}
N	0	0	X	1	0	0	1	0	X
C_2	0	1	0	1	1	0	1	0	$-V_{dc}$

$$\frac{e_A}{N_1} = \frac{e_{a_1}}{N_2} = \frac{e_{a_2}}{N_2} \tag{11}$$

$$i_A N_1 - i_{a_1} N_2 + i_{a_2} N_2 = 0 \tag{12}$$

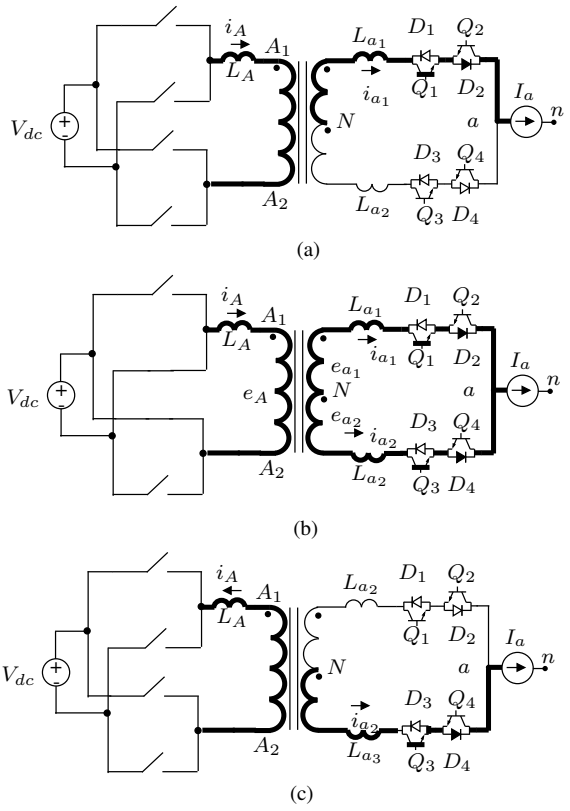

Fig. 4. Commutation

$$I_a = i_{a_1} + i_{a_2} \tag{13}$$

$$V_{dc} = L_A \frac{d}{dt} i_A + e_A \tag{14}$$

$$e_{a_1} + e_{b_1} = L_{a_1} \frac{d}{dt} i_{a_1} - L_{a_2} \frac{d}{dt} i_{a_2} \tag{15}$$

$$\frac{d}{dt} i_{a_2} = \frac{V_{dc} \left(\frac{N_2}{N_1} \right)}{\left(\frac{L_{a_1} + L_{a_2}}{2} \right) + 2 L_A \left(\frac{N_2}{N_1} \right)^2} \tag{16}$$

$$t_{com} = \left[\frac{\left(\frac{L_{a_1} + L_{a_2}}{2} \right) + 2 L_A \left(\frac{N_2}{N_1} \right)^2}{V_{dc} \left(\frac{N_2}{N_1} \right)} \right] I_o \tag{17}$$

III. Simulation

The entire topology as shown in Fig. 1 along with the suggested control has been simulated in MATLAB/Simulink. The various different parameters for the simulation are given in Table IV. Fig. 5 shows simulated output voltage, load current and current through the upper half of the secondary winding in phase A. The peak of the output current is little less than its analytically predicted value (Analytical $I_a = 29.46A$, Simulated $I_a = 28.90A$). This is due to voltage loss during commutation. Waveforms for one cycle of the signal S is

TABLE IV
Parameters

L_{load}	$10mH$
R_{load}	2.5Ω
L_{A,a_1,a_2}	$40\mu H$
R_{A,a_1,a_2}	0.2Ω
L_m	$15\ mH$
$\frac{N_2}{N_1}$	1
V_{dc}	500V
$f_s = \frac{1}{T_s}$	5kHz
ω_o	$2\pi 60$
m	0.4

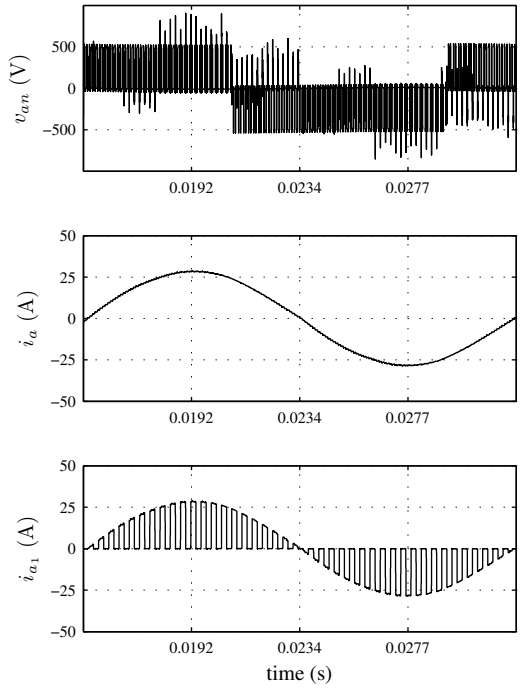

Fig. 5. Simulation result: a) output voltage b) output current c) current through the upper half of secondary winding

shown in Fig. 6. The current in the upper half of the phase a winding (waveform i_{a_1}) linearly changes to its desired value during C_1 and C_2 as predicted by (16). These slopes are in agreement with their analytical predictions. The magnetizing current of the transformer in phase a is shown as the waveform i_m. It confirms flux balance over one cycle of S. v_{cm} is the common-mode voltage waveform. It is zero except during commutation (when C_1 and C_2 are active). It is to be noted that here the available voltage for commutation is V_{dc}. It is double in comparison with that of the topology described in [9].

IV. Conclusion

In this paper, a new converter topology along with a novel control technique for a direct dc/ac conversion with a high frequency ac-link for three-phase PWM drives has been proposed. The proposed topology has the following extra

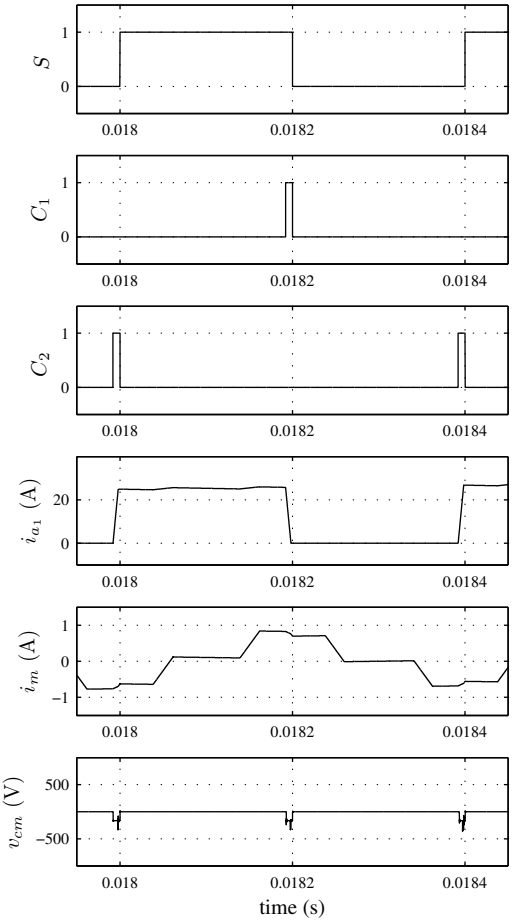

Fig. 6. Simulation results: Commutation

benefits when compared to a recently proposed, [9], drive with high frequency ac-link:

1) Reduced common-mode voltage switching (zero during power transfer and switches only once in cycle, during commutation)
2) High quality output voltage profile comparable to a two level inverter operated with CSVPWM.
3) The lossless commutation process of leakage energy has been simplified
4) Availability of more voltage for commutation implies, lower commutation time, higher frequency of operation and smaller size.

The converter has been analyzed in detail. It has been simulated with a non-ideal transformer by taking the leakage inductances into account. The presented simulation results verify the converter's operation and confirm the stated advantages. This is a promising topology for connecting renewable energy sources to HVDC grid.

REFERENCES

[1] V. John, N. Mohan, E. Persson, and R. Nilssen, "High frequency isolation in standby power supplies which compensate load harmonic currents," in *Industrial Electronics, Control, and Instrumentation, 1993. Proceedings of the IECON '93., International Conference on*, Nov 1993, pp. 1264–1268 vol.2.

[2] P. Krein, R. Balog, and X. Geng, "High-frequency link inverter for fuel cells based on multiple-carrier pwm," *Power Electronics, IEEE Transactions on*, vol. 19, no. 5, pp. 1279–1288, Sept. 2004.

[3] B. Ozpineci and B. Bose, "Soft-switched performance-enhanced high frequency nonresonant link phase-controlled converter for ac motor drive," in *Industrial Electronics Society, 1998. IECON '98. Proceedings of the 24th Annual Conference of the IEEE*, vol. 2, Aug-4 Sep 1998, pp. 733–739 vol.2.

[4] J. Gafford, M. Mazzola, J. Robbins, and G. Molen, "A multi-kilowatt high-frequency ac-link inverter for conversion of low-voltage dc to utility power voltages," in *Power Electronics Specialists Conference, 2008. PESC 2008. IEEE*, June 2008, pp. 3707–3712.

[5] S. Manias, P. Ziogas, and G. Oliver, "Bilateral dc to ac converter employing a high frequency link," in *Industry Applications Society Annual Meeting, 1985., Conference Record of the 1985 IEEE*, 1985, pp. 1156–1162.

[6] T. Kawabata, K. Honjo, N. Sashida, K. Sanada, and M. Koyama, "High frequency link dc/ac converter with pwm cycloconverter," in *Industry Applications Society Annual Meeting, 1990., Conference Record of the 1990 IEEE*, Oct 1990, pp. 1119–1124 vol.2.

[7] S. Deng, H. Mao, J. Mazumdar, I. Batarseh, and K. Islam, "A new control scheme for high-frequency link inverter design," in *Applied Power Electronics Conference and Exposition, 2003. APEC '03. Eighteenth Annual IEEE*, vol. 1, Feb. 2003, pp. 512–517 vol.1.

[8] M. Matsui, M. Nagai, M. Mochizuki, and A. Nabae, "High-frequency link dc/ac converter with suppressed voltage clamp circuits-naturally commutated phase angle control with self turn-off devices," *Industry Applications, IEEE Transactions on*, vol. 32, no. 2, pp. 293–300, Mar/Apr 1996.

[9] K. Basu, A. Somani, K. Mohapatra, and N. Mohan, "Three phase ac/ac power electronic transformer based pwm ac drive with loss less commutation of leakage energy," in *SPEEDAM 2010-PISA Italy*, June 2010.

[10] M. Baiju, K. Mohapatra, R. Kanchan, and K. Gopakumar, "A dual two-level inverter scheme with common mode voltage elimination for an induction motor drive," vol. 19, no. 3, May 2004, pp. 794–805.